Contents

Abstract . . . 3
List of Figures . . . 5

1 Test Case Description **7**
1.1 Introduction . . . 7
1.2 Apparatus and test case description . . . 7
1.3 Flow main features description . . . 7
1.4 Numerical code . . . 8
1.4.1 Numerical scheme . . . 8
1.5 Physical modeling . . . 9
1.5.1 Turbulence . . . 9
1.5.2 Transport . . . 9
1.5.3 Combustion . . . 9
1.5.4 Chemistry . . . 9
1.5.5 Modeling assumption . . . 9
1.6 Boundary conditions . . . 10
1.6.1 Plug test case . . . 10
1.6.2 Ducts test case . . . 10

2 Results **11**
2.1 Introduction . . . 11
2.2 Velocity profiles . . . 11
2.3 Turbulence intensity profiles . . . 12
2.4 Methane concentration profiles . . . 12
2.5 Results discussion . . . 12
2.6 Effects due to turbulence intensity . . . 13
2.7 Effects due to inlet mean velocity . . . 14
2.8 Grid refinement . . . 14
2.9 Conclusions . . . 14

Bibliografy **27**

Abstract

This report presents results of computational simulations of a premixed combustion flow in an experimental plane combustor.
In Chapter 1 a brief description of the test case and of flow main characteristics are given.
Results obtained from computations are compared each others and with experimental results in Chapter 2.
Finally, results are discussed and conclusions on results quality are drawn.

List of Figures

1.1 Moreau-Boutier experimental apparatus. Figure taken from Ref. [4]. 8

2.1 Mean velocity profiles at 39 mm from inlets: comparison with experimental data. 16
2.2 Mean velocity profiles at 151 mm from inlets: comparison with experimental data. 16
2.3 Mean velocity profiles at 351 mm from inlets: comparison with experimental data. 17
2.4 Mean velocity profiles at 650 mm from inlets: comparison with experimental data. 17
2.5 Comparison between calculations and experiments for CH_4 molar fractions scaled using N_2 molar fractions: profiles at 22 mm from inlet. 18
2.6 Comparison between calculations and experiments for CH_4 molar fractions scaled using N_2 molar fractions: profiles at 522 mm from inlet. 18
2.7 Turbulent rate and velocity fluctuation in x direction: profiles measured at different axial sections. Figure taken from Ref. [4]. 19
2.8 Ratio between velocity fluctuation and mean velocity in x direction: profiles calculated at different axial sections. 20
2.9 Velocity fluctuation in x direction: profiles calculated at different axial sections. 21
2.10 Mean velocity profiles at 39 mm from inlet: comparison for different inlet levels of turbulent intensity (10, 15, 20 %). . . 21
2.11 Mean velocity profiles at 650 mm from inlet: comparison for different inlet levels of turbulent intensity (10, 15, 20 %). . . 22
2.12 Velocity fluctuation profiles at 39 mm from inlet: comparison for different inlet levels of turbulent intensity (10, 15, 20 %). . 22
2.13 Velocity fluctuation at 650 mm from inlet: comparison for different inlet levels of turbulent intensity (10, 15, 20 %). 23

2.14 Turbulence intensity profiles at 39 mm from inlet: comparison for different inlet levels of turbulent intensity (10, 15, 20 %). . 23
2.15 Turbulence intensity profiles at 650 mm from inlet: comparison for different inlet levels of turbulent intensity (10, 15, 20 %). . 24
2.16 CH_4 concentration profiles at 650 mm from inlet: comparison for different inlet levels of turbulent intensity (10, 15, 20 %). . 24
2.17 Mean velocity profiles at 39 mm from inlet: comparison for different values of inflow velocity. 25
2.18 Mean velocity profiles at 650 mm from inlet: comparison for different values of inflow velocity. 25

Chapter 1

Test Case Description

1.1 Introduction

The test case considered in this report is described in details in Refs. [4] and briefly presented in the following.

1.2 Apparatus and test case description

The combustor is a plane experimental combustor feeded with two flows: the former is a homogeneous unburnt mixture of CH_4 and Air with equivalence fuel ratio $\phi = 0.8$, and the latter is a burned CH_4-air stoichiometric mixture ($\phi = 1$). A schematic of the experimental apparatus is shown in Fig. 1.1. Overall dimensions of the combustor are hight .10 m (the combustor section is a square) and length 1.3 m. The two inlet flows are divided by a splitter plate: the burned gas inlet is .02 m high, the fresh mixture inlet .08 m high. The chamber walls are uncooled and equipped with probes to measure temperature and chemical species concentrations during the test. Each test lasts for 30 seconds.

1.3 Flow main features description

The burned gas entering from the lower inlet ignites the fresh mixture and stabilizes the flame which then propagates along the combustor. The flow regime is turbulent and, for the range of velocities ($55 \div 200$ m/s) and turbulence intensity ($< 20\%$) explored, no recirculations are expected.

It has been found that the velocity gradient between cold and hot flow favors the combustion efficiency [4]. A test case with the two flows at the

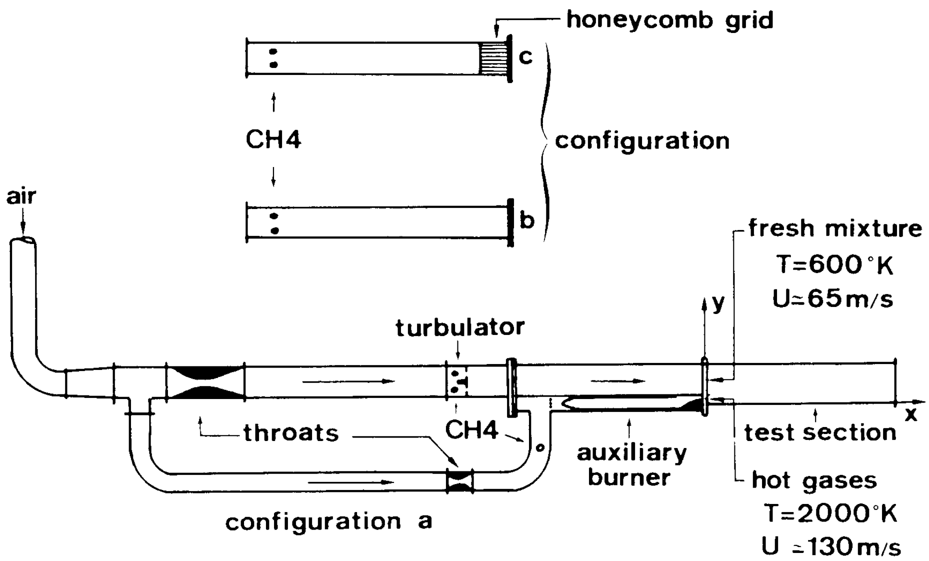

Figure 1.1: Moreau-Boutier experimental apparatus. Figure taken from Ref. [4].

same velocity led to fresh mixture ignition but the flame developed more slowly. Therefore the pilot flow as been run at twice the velocity of the fresh mixture.

Turbulence has been found to affects much the flame behavior, in fact experiments showed that increasing inlet turbulence yields to better combustion. Inlets levels of turbulence found for cold run increase of $1 \div 3\%$ when combustion occurs. This has been attributed to experimental apparatus mechanical vibrations.

1.4 Numerical code

The numerical code used for the simulations presented in this report is the GT-TURBO_EDC, 2D-axisimetric code suitable for incompressible flows including combustion in both premixed and non-premixed regime.

The code is based on the SIMPLE algorithm [5] and uses non-staggered grids thanks to the application of a Rie-Chow interpolation.

1.4.1 Numerical scheme

For the discretization of convective-diffusive fluxes the "hybrid scheme" is used [5].

1.5 Physical modeling

1.5.1 Turbulence

A standard $k - \epsilon$ model plus wall functions have been used.

1.5.2 Transport

Diffusion coefficients are assumed to be the same for all chemical species, and the Lewis number is assumed equal one ($Le = 1$). Gas mixture laminar viscosity is calculated using Sutherland law.

1.5.3 Combustion

The combustion model used is the Eddy Dissipation Concept by Magnussen [3] coupled with a Perfect Stirred Reactor solver taken from the CHEMKIN package [2].

1.5.4 Chemistry

Several chemistry models based on reduced chemical kinetics mechanisms have been tested on the `GTTURBO_EDC`. In this report the base test case has been calculated using the 6-steps reduced chemistry mechanism for CH_4-air combustion proposed by Chang and Chen [1].

1.5.5 Modeling assumption

In this report the simulation has been performed assuming:

- two-dimensional flow simulations suitable;
- adiabatic flow (negligible thermal exchange at combustor walls);
- non catalytic walls;
- radiation effects negligible.

Table 1.1: Test case characteristics

Flow regime	turbulent
Combustion regime	premixed
Fuel	CH_4
Oxidizer	air
Pressure	1 atm
ϕ_u	0.8
ϕ_b	1.0
Geometry	plane
Unburnt gas velocity (m/s)	65
Burnt gas velocity (m/s)	130
Unburnt gas temp (K)	600
Burnt gas temp (K)	~ 2000

1.6 Boundary conditions

Boundary conditions for the "base" test case have been set up taking the mean velocity and equivalence ratios suggested by the experimentalists (see Table 1.5.5). A level of turbulence of 10% has been assumed as starting approximation.

1.6.1 Plug test case

In this case the computational domain coincides with the combustion chamber and the boundary conditions are imposed directly at its entrance. Uniform boundary conditions (flat profiles) for all vectorial and scalar quantities have been imposed at the entrance of the combustor.

1.6.2 Ducts test case

In this case the computational domain is formed by the combustion chamber plus two inlet ducts one for the burnt mixture and one for the unburnt mixture. In this case inlet boundary conditions are imposed at the entrance of each ducts as flat profiles for all vectorial and scalar quantities. Results for this kind of boundary conditions will be presented in a future Report.

Chapter 2

Results

2.1 Introduction

These simulations are suited to reproduce the base test case referred to the experimental results of Moreau an Boutier [4]. A summary of boundary conditions used can be found at the end of this Chapter in the Table 2.9. Notice in the figures capital letters without apex stay for averaged quantities (mean velocities, etc.), while U' stays for $\sqrt{\overline{u'^2}}$.

2.2 Velocity profiles

Figures 2.1 - 2.4 show comparisons between calculated (lines) and experimental (dots) mean velocities taken at several section along the combustor.

A fair agreement has been found for the first two profiles (see Figs. 2.1 and 2.2) specially for the unburned part of the flow. A visible difference exists for the mean velocity in the lower part of the combustor. Figure 2.1 show also that the plug boundary conditions used at the inlets cannot follow the minimum of mean velocity coming from the matching of the two boundary layers after the splitter plate.

Moving downstream along the combustor the calculated velocities show a increasing disagreement with respect to experiments (see Figs.2.3 and 2.4). For the section at 650 mm from inlets, the peak mean velocity is 16 % lower than the experimental one whereas in the middle of the combustor the difference rises to 37 %.

To understand and explain these large differences, is better to have a look to the turbulent characteristics of the flow.

2.3 Turbulence intensity profiles

Figures 2.8 and 2.9 show turbulent intensity and velocity fluctuations profiles taken at several sections along the combustor. Experimental values of the same quantities taken from Ref. [4] are reported in Figs. 2.7 and **??**. Comparisons of these data show that already in the section nearest to the inlets the calculated levels of turbulent intensity are too low with respect to the experiments. In fact looking to the profiles reported in Ref. [4] we see that unburned flow turbulence intensity is of $\sim 13\%$ and burned flow turbulence intensity is $> 18\%$. In our results the peak of turbulence intensity due to the presence of the shear layer is correctly placed but the value is 40 % lower. Downstream along the combustor, the peak of turbulence intensity is mainly due to the transverse velocity gradient located in correspondence of the zone of intense chemical reactions; its position rises following the rise of the flame front. This is not reproduced by the calculations where the maximum rises very slowly and remains located in the lower half of the combustor even for the farthest section (see Fig. 2.9).

2.4 Methane concentration profiles

Figures 2.5 and 2.6 show the transverse profiles of CH_4 molar fractions scaled using N_2 molar fractions at 22 and 522 mm from inlet.

A fair agreement has been found at the first section even thought the calculation gives a too small CH_4 concentration just below the splitter plate. A very different scenario has been found on the farther section where experiments show much more fuel consumption in the higher part of the combustor. This in agreement with what already said, shows as the simulation gives a less intense combustion due to the too small flame angle.

2.5 Results discussion

The large difference existing between the calculated results and the experimental data can be due to several factors. One is the correctness of boundary conditions imposed at inlets for the calculations. The difference between the turbulence levels has been already underlined in the previous Section. Another difference seems to exist for the burned gas axial mean velocity. Looking at Fig. 2.1 we see that already at 39 mm from inlet the experimental velocity is much lower than the calculated one. This let the author think that a much more suitable value for the burned flow mean velocity could be $\sim 110 m/s$.

Furthermore, from the numerical results presented the author concludes that the combustion model seems to give a poorer combustion which regard to the experiments. This can be seen looking at the velocity profiles at the farthest sections (see Figs. 2.3 and 2.4) and at the turbulence intensity profile which show the maxima located in the lower half part of the combustion section (see Fig. 2.8). In fact, assuming the turbulent rate be maximum in the combustion zone leads to a calculated flame front too flat (low turbulent flame velocity).

Before drawing final conclusions about the effectiveness of the combustion model, some further tests have to be done to check grid independence and, much more important, new boundary conditions which reproduce better real flow conditions.

2.6 Effects due to turbulence intensity

Results on turbulence intensity measured in the experiment and reported in Fig. 2.7 show two main characteristics: turbulence levels of the two inlet flows are different and both are higher than 10%. This lead to inquire the effect of changing inlet turbulent intensity on the combustion flow simulation. Inlet turbulence levels has been varied from 10 up to 20% for both cold and hot flows. Results are shown by Figs. 2.10 – 2.15.

Figure 2.10 shows a very little influence on the velocity profiles at the section nearer to the inlets (39 mm), the peak of velocity in the hot flow is unchanged as far as the unburned flow mean velocity. Small differences exist in the splitter plate wake.

Fig. 2.11 shows that a more sensitive effect can be found downstream in the combustor. The calculated profiles of mean velocity tend to became nearer to the experimental ones but, even for turbulence intensity of 20 %, the disagreement is still large.

From Fig. 2.14 we see that, changing the turbulent intensity in inlet, calculations give results which move towards experiments.

Figures 2.11 and 2.15 can be used to observe the effects of inlet turbulent intensity on combustion. The former shows as the combustion effectiveness rises whit inlet turbulent intensity but looking at the latter we can see a very poor movement of the turbulent intensity maximum. This means that the flame front does not changes its angle very much, i.e. the turbulent flame velocity is almost the same in the three cases. To further verify, for this same combustor position, $CH4$ consumptions are compared in Figure 2.16: even thought the increased turbulence level increases the CH_4 consumption, i.e. the combustion efficiency, the position of the flame in this section does not change very much and remains still far from the expected one.

2.7 Effects due to inlet mean velocity

Figure 2.17 shows a comparison between experiments and calculated mean velocity profiles obtained changing the inlet mean velocity value. The test case used is the one with inlet turbulent intensity set to 20%. The dashed line is the profile obtained using 110 m/s at inlet. It is evident how at 39 mm from inlet the difference underlined in one of the previous sections can be recovered with a lower inflow velocity for the burned gas. The same calculations are compared in Fig. 2.18 at 650 mm: the smaller inlet velocity for the burned gas lowers the peak of mean velocity in this section making the disagreement between experiments and calculations larger.

These results will be accounted for to set up the new test case boundary conditions.

2.8 Grid refinement

No grid refinement comparison is available for this report.

2.9 Conclusions

After examining the results presented the author concludes that the inflow velocity for the burnt gas should be assumed $\sim$ 110 m/s instead than 130 m/s. A suitable assumption for inlet turbulent intensity could be 13% for the unburnt gas flow and 18% for the burnt gas flow. Starting from these new inlet conditions the computational results will produce more clear evidence about the effectiveness of the combustion model used. Therefore conclusions on needs to combustion model tuning can be drawn only after further simulations.

Table 2.1: Boundary conditions for plug test case: CASE 1

	Burnt gas inlet	Unburnt gas inlet
u (m/s)	130.0	65.0
v (m/s)	.0	.0
w (m/s)	.0	.0
turb. int.	10 %	10 %
k (m^2/s^2)	253.5	63.37
$\mathcal{L}$ (m)	.2	.8
λ	.1	.1
ϵ		
ϕ	1.0	.8
Y_{CO_2}	.11177	.0
Y_{H_2O}	.10624	.0
Y_{CO}	.02084	.0
Y_{O_2}	.01612	.233
Y_{OH}	.00520	.0
Y_{H_2}	.00074	.0
f	.05500	.04450

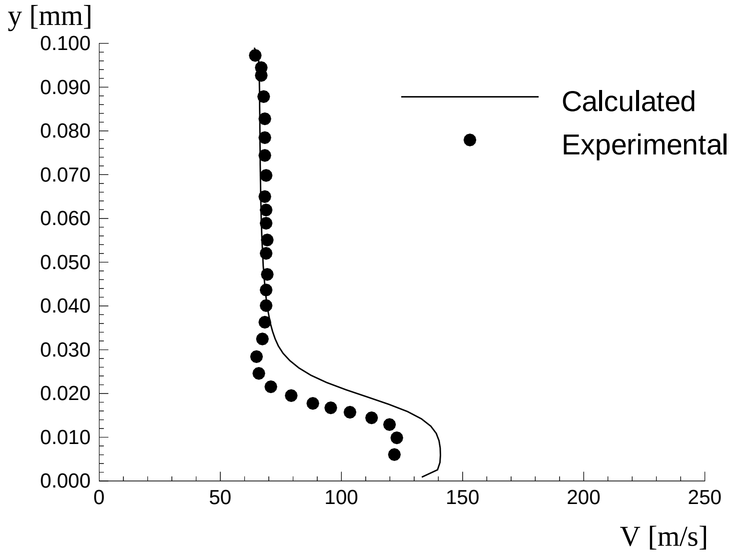

Figure 2.1: Mean velocity profiles at 39 mm from inlets: comparison with experimental data.

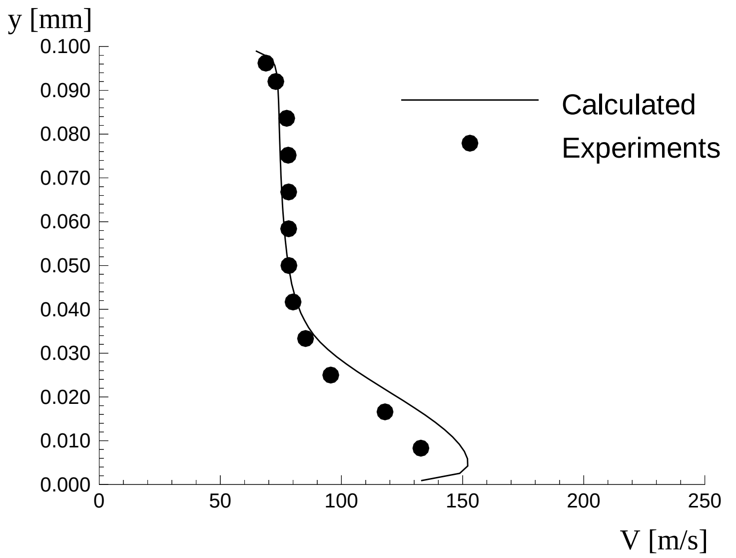

Figure 2.2: Mean velocity profiles at 151 mm from inlets: comparison with experimental data.

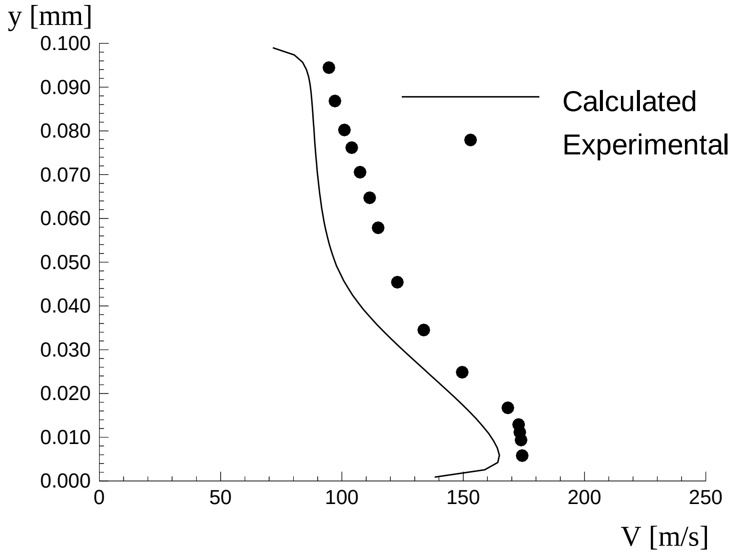

Figure 2.3: Mean velocity profiles at 351 mm from inlets: comparison with experimental data.

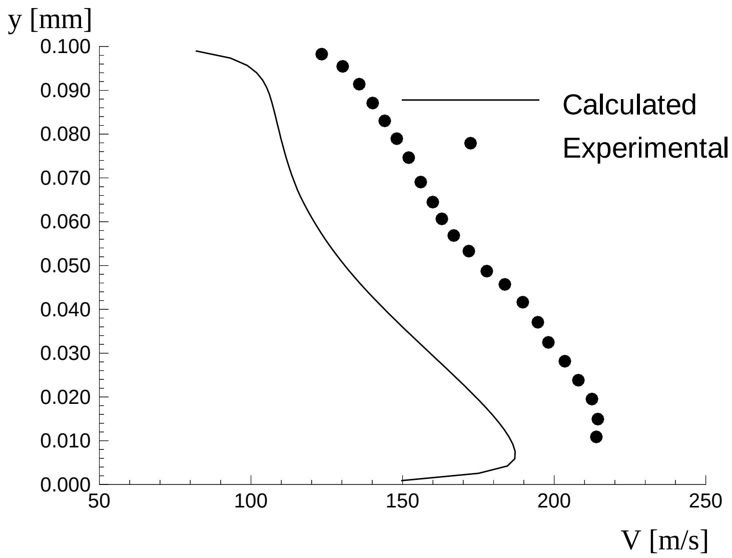

Figure 2.4: Mean velocity profiles at 650 mm from inlets: comparison with experimental data.

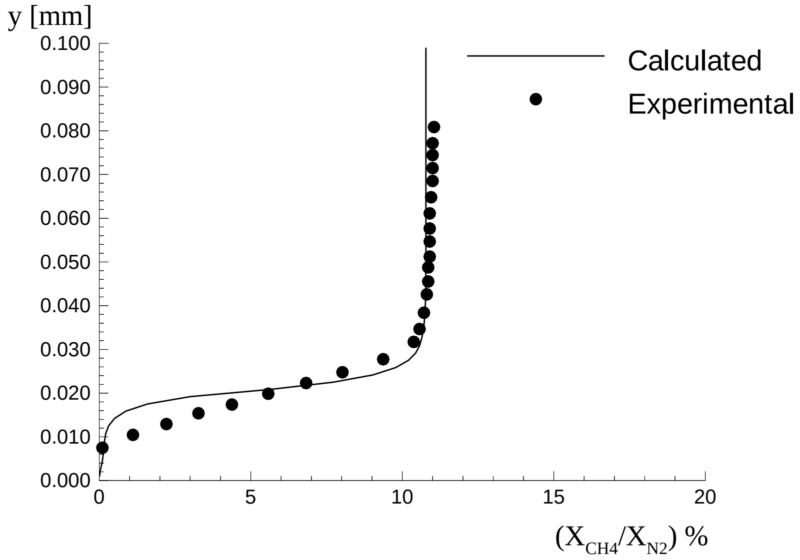

Figure 2.5: Comparison between calculations and experiments for CH_4 molar fractions scaled using N_2 molar fractions: profiles at 22 mm from inlet.

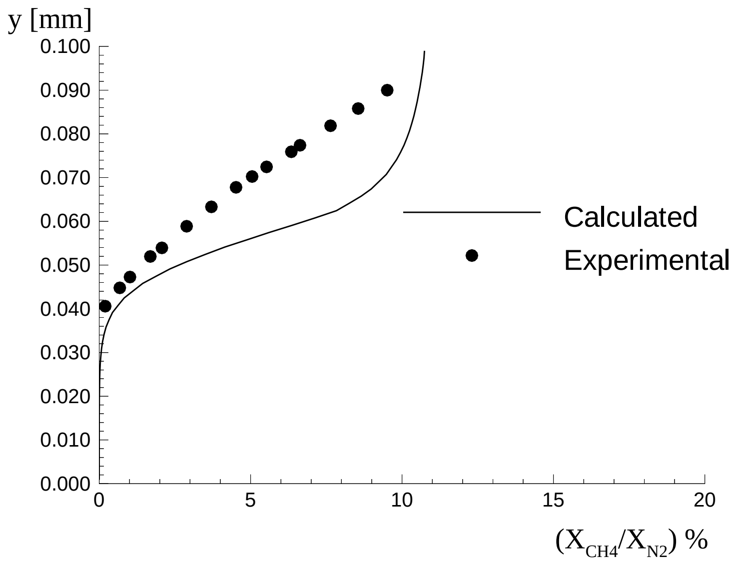

Figure 2.6: Comparison between calculations and experiments for CH_4 molar fractions scaled using N_2 molar fractions: profiles at 522 mm from inlet.

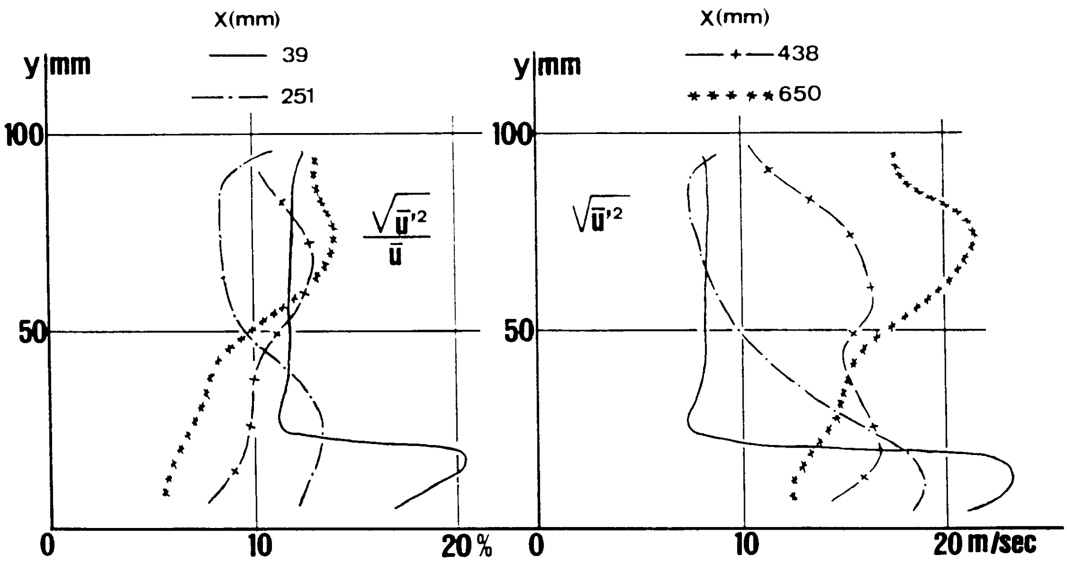

Figure 2.7: Turbulent rate and velocity fluctuation in x direction: profiles measured at different axial sections. Figure taken from Ref. [4].

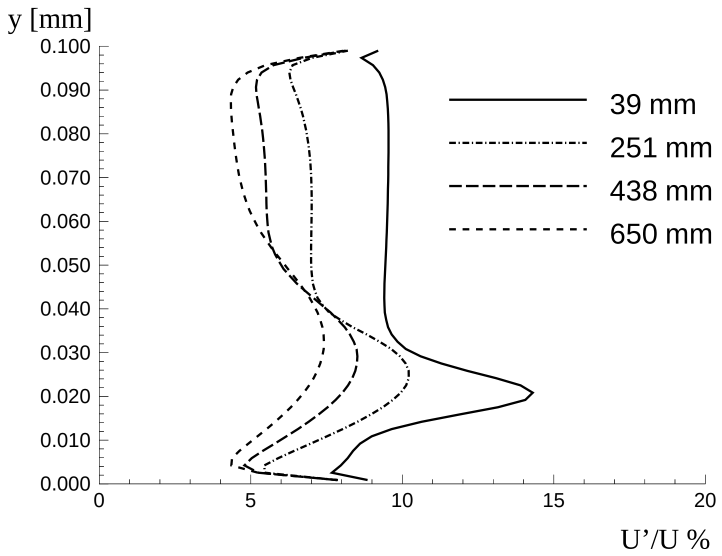

Figure 2.8: Ratio between velocity fluctuation and mean velocity in *x* direction: profiles calculated at different axial sections.

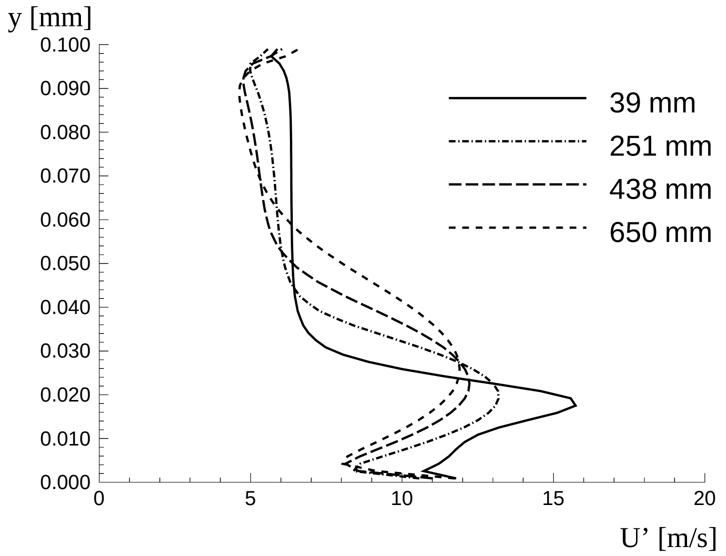

Figure 2.9: Velocity fluctuation in x direction: profiles calculated at different axial sections.

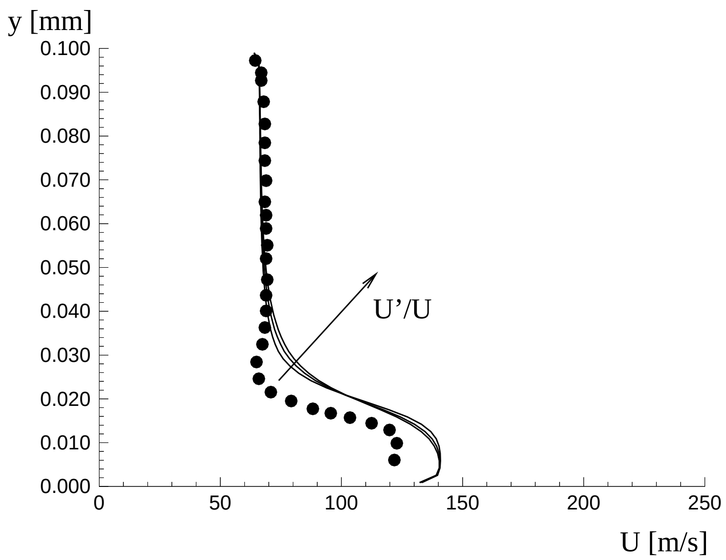

Figure 2.10: Mean velocity profiles at 39 mm from inlet: comparison for different inlet levels of turbulent intensity (10, 15, 20 %).

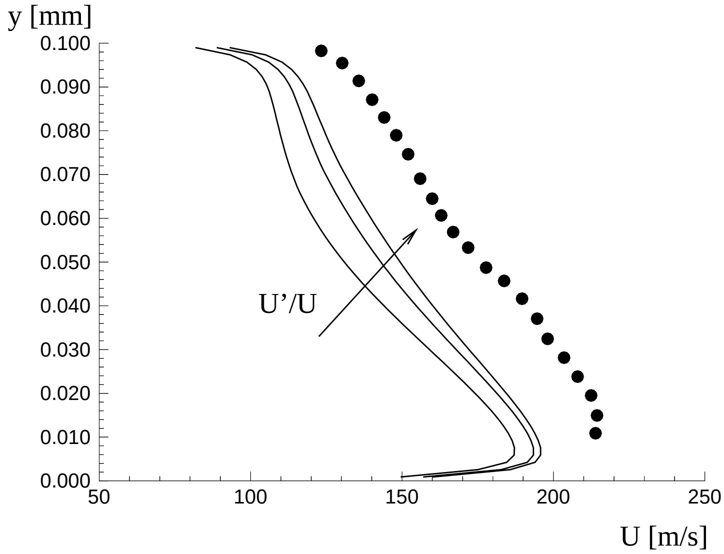

Figure 2.11: Mean velocity profiles at 650 mm from inlet: comparison for different inlet levels of turbulent intensity (10, 15, 20 %).

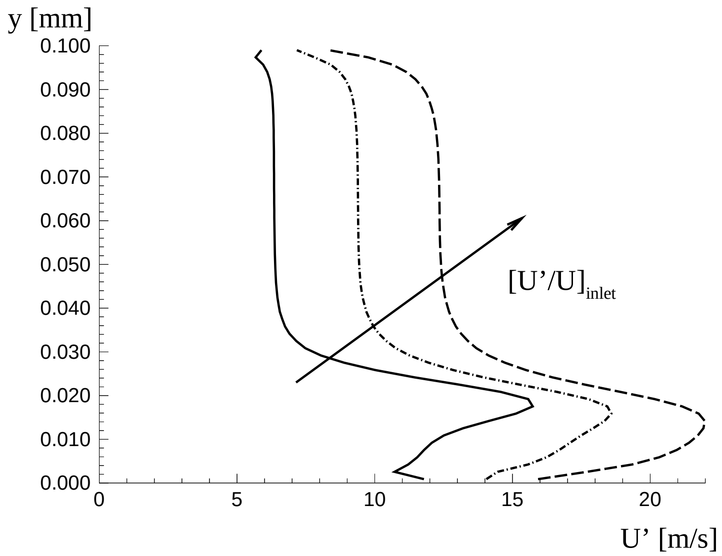

Figure 2.12: Velocity fluctuation profiles at 39 mm from inlet: comparison for different inlet levels of turbulent intensity (10, 15, 20 %).

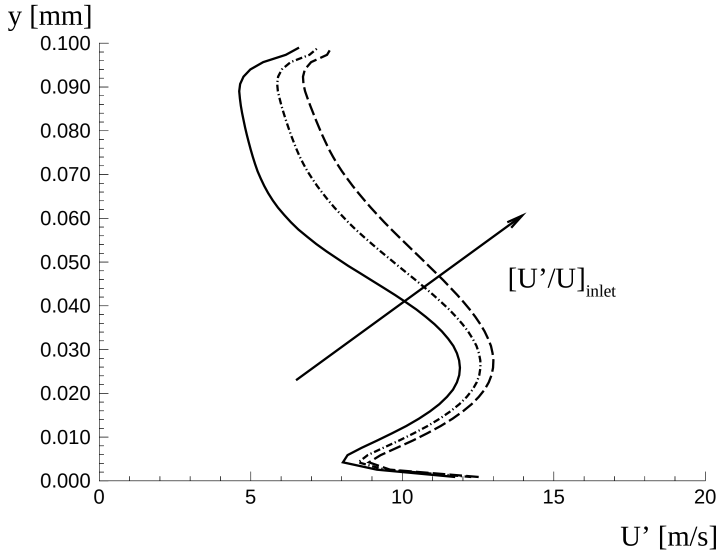

Figure 2.13: Velocity fluctuation at 650 mm from inlet: comparison for different inlet levels of turbulent intensity (10, 15, 20 %).

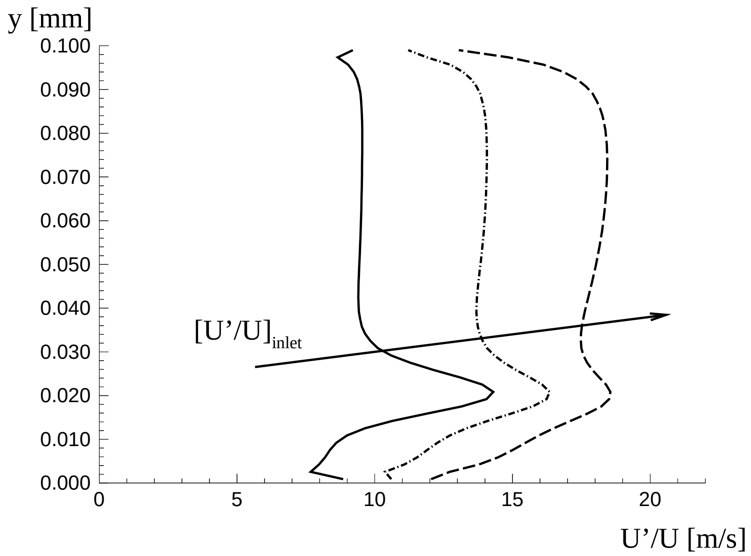

Figure 2.14: Turbulence intensity profiles at 39 mm from inlet: comparison for different inlet levels of turbulent intensity (10, 15, 20 %).

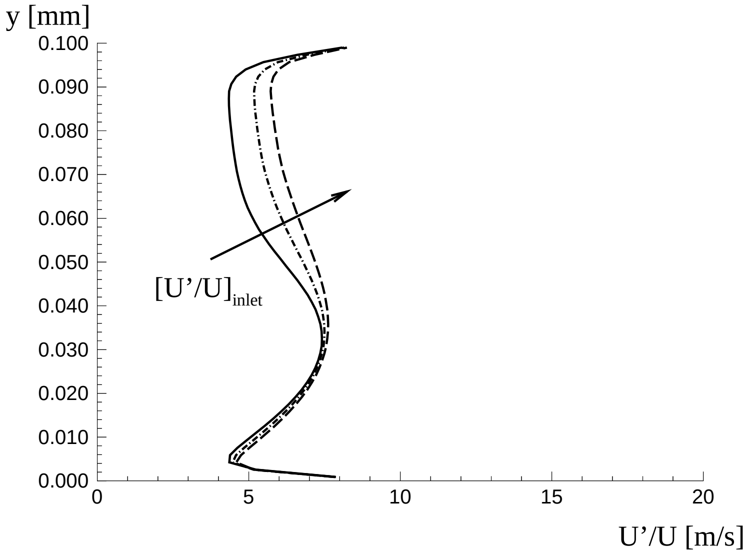

Figure 2.15: Turbulence intensity profiles at 650 mm from inlet: comparison for different inlet levels of turbulent intensity (10, 15, 20 %).

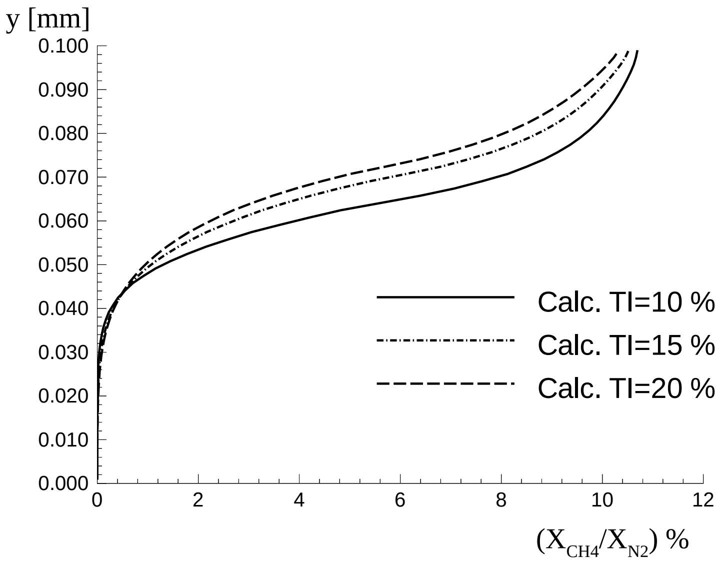

Figure 2.16: CH_4 concentration profiles at 650 mm from inlet: comparison for different inlet levels of turbulent intensity (10, 15, 20 %).

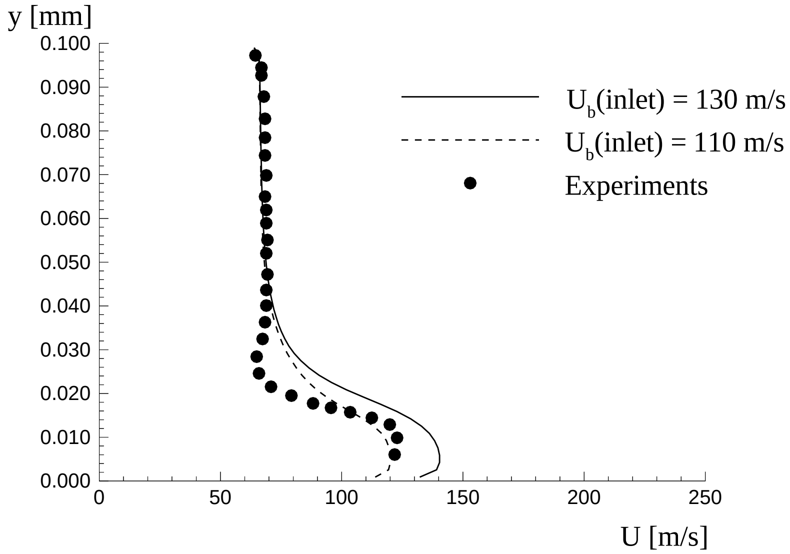

Figure 2.17: Mean velocity profiles at 39 mm from inlet: comparison for different values of inflow velocity.

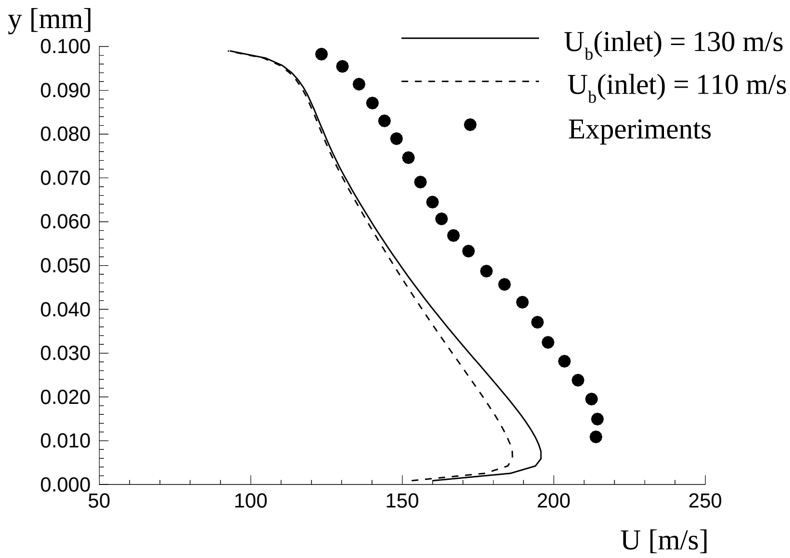

Figure 2.18: Mean velocity profiles at 650 mm from inlet: comparison for different values of inflow velocity.

Bibliography

[1] Chang, W.C. and Chen, J.-Y. Reduced Reaction Mechanism for the Oxidation of CH_4 Lean Flames. *http://firefly.berkeley.edu/griredu.html*, 1990.

[2] Glaborg, P., Kee, R.J., Grcar, J.F., and Miller, J.A. PSR: A Fortran Program for Modeling Well-Stirred Reactors. Technical Report SAND86-8209 UC-4, SANDIA National Laboratories, Reprinted Nov. 1993.

[3] Magnussen, B.F. The Eddy Dissipation Concept for Turbulent Combustion Modeling. Its Physical and Practical Implications. *XI Task Leaders Meeting – Energy Conservation in Combustion, IEA*, 1989.

[4] Moreau, P., and Boutier, A. Laser Velocimetry Measurements in a Turbulent Flame. In *Sixteenth Symposium (International) on Combustion*, pages 1747–1756. The Combustion Institute, 1976.

[5] Patankar, S.V. *Numerical Heat Transfer and Fluid Flow*. Hemisphere Publishing Corporation, New York, 1980.